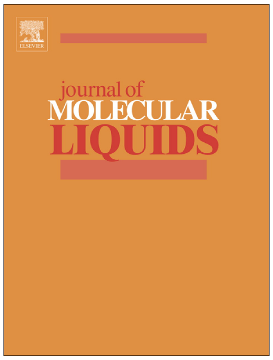

# Investigation on environmental sensitivity characteristics of pyridine compounds with different position of N-atoms and various active functional groups

M. Khadem Sadigh, M.S. Zakerhamidi, A.N. Shamkhali, B. Shaabani, N. Rad-Yousefnia

PII: S0167-7322(18)34492-1
DOI: https://doi.org/10.1016/j.molliq.2018.11.090
Reference: MOLLIQ 10000

To appear in: *Journal of Molecular Liquids*

Received date: 30 August 2018
Revised date: 16 November 2018
Accepted date: 19 November 2018

Please cite this article as: M. Khadem Sadigh, M.S. Zakerhamidi, A.N. Shamkhali, B. Shaabani, N. Rad-Yousefnia , Investigation on environmental sensitivity characteristics of pyridine compounds with different position of N-atoms and various active functional groups. Molliq (2018), https://doi.org/10.1016/j.molliq.2018.11.090

# Investigation on environmental sensitivity characteristics of pyridine compounds with different position of N-atoms and various active functional groups

*M. Khadem Sadigh[a], M. S. Zakerhamidi[a], A. N. Shamkhali[b,c], B. Shaabani[d], N. Rad-Yousefnia[d]*

*[a]Research Institute for Applied Physics and Astronomy, University of Tabriz, Tabriz, Iran*

*[b]Department of Chemistry, Faculty of Science, University of MohaghegArdabili, 56199-11367 Ardabil, Iran*

*[c]Neuroscience Research Center, Iran University of Medical Sciences, Tehran, Iran*

*[d]Department of inorganic Chemistry, Faculty of chemistry, University of Tabriz, Tabriz, Iran*

* Corresponding Author
Mahsa Khadem Sadigh
Tel: number: +98-41-33393027
Fax: number: +98-41-33347050
E-mail: mahsa.sadigh@tabrizu.ac.ir , mahsa.sadigh@yahoo.com

## Abstract

Environment induced effects including polarity play important role in controlling physical, biological, and chemical behavior of local molecules. In this study, due to the importance of this issue, solvatochromism and charge transfer characteristics of some groups of pyridine compounds were investigated in various environments with different polarity. According to the experimental results, polarity of molecular surrounding environment, position of N-atom in pyridine rings, and various active functional groups have profound effects on the molecular photo-physical features.

The contribution of various solvent induced effects on the solvatochromism characteristics of samples were also investigated by using of linear salvation energy relationship concept. Moreover, according to the experimental data and density functional theory calculations, the differences between molecular dipole moment values in the ground and excited states are high enough to increase the probability of charge transfer mechanism. Therefore, from the theoretical calculations and quantitative experimental results of solute-solvent various interactions' contributions, it is possible to estimate the operation of pyridine compounds in various physical, chemical and biological phenomena in the solvent media.

**Keywords:** Photo-physical, Pyridine, Solvent polarity, Solute-solvent interaction, Dipole moment, Density functional theory

## 1. Introduction

The compounds containing pyridine ring, nitrogen comprising six membered aromatic rings, have gained intense attention during the last years. These materials with interesting characteristics play major roles in metabolism [1]. Furthermore, these compounds can be used as precursor for synthesis of pesticides [1-2], ligand in coordination chemistry [2] and anti-cancer agents [3-5]. In addition to the mentioned characteristics, they are found widely in pharmaceuticals [6], dyestuffs [2] and electronic devices [7]. First derivate of pyridine was acquired from coal tar by Anderson in 1846 [8].Then different methods were provided by Ramsay [9], Hantzsch [10] and Chichibabin [11] for synthesis of pyridine and its derivatives. Because of their importance, they are still used in industrial processes.

Various factors can modify the operation of pyridine compounds in various biological, physical and chemical phenomena. Molecular surrounding media features as one of the most fundamental factors can have considerable effects on the various phenomena. In real, the majority of experimental works and natural phenomena are usually performed in the solution state. In this case, different molecular interactions can play important roles on the response of solute molecule in various phenomena. These interactions are divided into two different types called specific and nonspecific interactions.

In general, solvent induced effects are usually studied by means of solvatochromic and solvent polarity parameters [12]. There are various physical, chemical and biological processes that single solvent polarity scales cannot explain completely the nature and degree of different solute-solvent interactions. Therefore, multi-parameter polarity parameters based on general multi-linear expression (equation (1)) are used [12].

$$y = y_0 + aA + bB + cC \tag{1}$$

In equation (1), $y_0$ describes the physicochemical property of understudy quantity in the reference solvent or gas phase. *a*, *b* and *c* coefficients also indicate the solvent dependent characteristic of understudy quantity (y) based on solvent polarity parameters (*A*, *B*, *C*).Two well-known sets of multi-parameter solvent polarity scales are proposed and formulated as Kamlet-Abboud-Taft and Catalan equations. Based on Kamlet-Abboud-Taft equation, *A*, *B* and *C* solvent polarity parameters indicate hydrogen bond donor (HBD) acidity ($\alpha$) [13], hydrogen bond acceptor (HBA) basicity ($\beta$) [14] and dipolarity/polarizability ($\pi^*$) [15], respectively. On the other hand, in Catalan formulation, *A*, *B* and *C* describe acidity (SA), basicity (SB) and polarity/polarizability (SPP) [16-17] of selected solvents.

In addition to molecular surrounding environment features, molecular electronic structure, molecular charge distribution characteristics and intra- and intermolecular interactions can be depend on the position of atoms in the aromatic rings and active functional groups in the molecular structures of selected samples.

Unfortunately, during the last years, it has not been reported a comprehensive experimental and TDDFT study on the selected materials in various solvent media with different polarity. Our aim of this work is investigation of media polarity effects on the linear optical properties and dipole moment characteristics of pyridine compounds. In this case, at first, solvatochromism behavior of pyridine compounds is studied at room temperature by UV-Visible spectroscopic technique. Then observable spectral shifts accompanied with theoretical methods are used for calculation of molecular dipole moments in the ground and excited states. By using these experimental and theoretical data for interactional behavior of pyridine compounds, it is possible to estimate the molecular dominant resonance structures and their operation in various physical, chemical and biological phenomena in solvent media.

## 2. Experimental

### *2.1. Materials*

In this work, the pyridine compounds were synthesized according to the common methods in the laboratory as follows:

Sample I: The compound 1 was prepared according to a literature method [18]. First, 2 ml of methanol solution of 4-pyridinecarboxaldehyde (1.88 ml, 20.0 mmol) was drop-wise added to a 10 ml methanol solution of 3-aminobenzoicacid (2.74 g, 20.0 mmol). Then, the mixture was refluxed for about 3 h. The acquired solid product was filtrated and washed with methanol before drying in air. Yield: 61% (1.54 g). FT-IR (KBr, cm$^{-1}$): 3443(m), 2885 (w), 1696 (s), 1608 (s), 1411(m), 1298 (vs), 1267 (s), 1229 (m), 1201(m), 1076 (m), 1048(m),824(m).

Sample II: The compound 2 was prepared according to a literature method [19-21]. First, 20.0 mmol (1.88 ml) of 4-pyridinecarboxaldehyde in 5 ml acetonitrile was added drop-wise to an acetonitrile solution of 1, 4-phenylendiamine (1.08 g, 10.0 mmol). Then, the mixture was stirred for about 3 h at room temperature. The formed solid product was separated and filtered off, and washed with acetonitrile (3-5 ml) and hexane (3-5 ml). Finally, it was dried in air to give sample II. Yield: 78% (2.23 g). FT-IR (KBr, $cm^{-1}$): 3028 (w), 2921 (w), 2888 (w), 2855 (w), 1627 (s), 1595 (s), 1551 (s), 1486 (s), 1412 (s), 1323 (s), 1221 (m), 1191(s), 1100 (m), 984 (w), 891 (m), 815 (s), 603 (m).

Sample III: The compound 3was prepared according to a literature method [22-23]. This sample was also prepared with the similar method to the synthesis of sample II, except that 3- pyridine carboxaldehyde (20.0 mmol, 1.88 ml) was added instead of 4-pyridinecarboxaldehyde. Yield: 68% (1.95 g). FT-IR (KBr, $cm^{-1}$) = 2924 (w), 2887 (w), 1619 (s), 1570 (s), 1489 (m), 1422 (m), 1363 (w), 1330 (w), 1287 (w), 1236 (w), 1194 (m), 1129 (w), 1104(w), 1022 (m), 973 (w),881 (m), 836 (s), 800 (m), 701 (s).

Moreover, the selected solvents with high purity were prepared from Merck. The solvent polarity parameters and polarity functions of them were also summarized in Table 1 [12, 16].

## *2.2. Absorption and emission spectroscopy*

First, diluted pyridinesolutions were prepared in selected solvents with diverse polarity. In real, for investigation of solute-solvent interaction effects and regardless of solute-solute interactions, the diluted sample solutions were prepared. Then, two spectroscopic devices were used for investigation of absorption and emmesion spectra of pyridine solutions.Double beam Shimadzu UV-2450 Scan Spectrophotomete is used for recording absorption spectra and JASCO FP-6200

Spectrofluorometer was selected for studying emession characteristics of samples.In this case, the optical length of quartz rectangular cuvettes for measurements were about 1 cm.

*2.3. Calculation of ground and excited state dipole moments*

The values of samples' dipole moments give important information about their geometrical structures and charge distribution features. In addition, this parameter can be useful for designing of nonlinear materials. Various procedures such as fluorescence polarization [24], Stark splitting [25], electric dichroism [26], microwave conductivity [27] and solvatochromism method [28-29] can be used for calculation of dipole moment values. Among the mentioned methods, the method based on solvent induced spectral shifts is usually used due to its simplicity. In this case, Kawaski et al. [30-31] by using of quantum mechanical perturbation theory expressed simple expressions for relation between solvent polarity parameters and difference and sum of maximum absorption and fluorescence wavelengths (in $cm^{-1}$) in diverse solvent environments. Such solvent dependent relations can be written according to the Eq. 2 and 3.

$$\upsilon_a - \upsilon_f = m_1 \; f(\varepsilon, n) + const. \quad (2)$$

$$\upsilon_a + \upsilon_f = -m_2 \, [\, f(\varepsilon, n) + 2g(n)] + const. \quad (3)$$

By definition of solvent polarity functions in the form of Eq. (4) and (5) and linear relation between the difference and sum of maximum wave numbers and solvent polarity functions, it is possible to obtain $m_1$ and $m_2$ slopes (Eq. (6) and (7)) .

$$f\left(\varepsilon,n\right)=\frac{\frac{\varepsilon-1}{2\varepsilon+1}-\frac{n^2-1}{2n^2+1}}{\left(1-\frac{2\alpha}{a^3}\frac{\varepsilon-1}{2\varepsilon+1}\right)\left(1-\frac{2\alpha}{a^3}\frac{n^2-1}{2n^2+1}\right)^2} \quad (4)$$

$$g(n)=\frac{\frac{n^2-1}{2n^2+1}\left(1-\frac{\alpha}{n^2}\frac{n^2-1}{2n^2+1}\right)}{1-\frac{\alpha}{a^3}\frac{n^2-1}{2n^2+1}} \quad (5)$$

$$m_1=\frac{2(\mu_e-\mu_g)^2}{hca^3} \quad (6)$$

$$m_2=\frac{2(\mu_e^2-\mu_g^2)}{hca^3} \quad (7)$$

In these relations, *ε, n, a*, and α symbols indicate dielectric permittivity, refractive index, spherical cavity radius of solute and average polarizability, respectively.

For an isotropic polarizability of solute molecule, the condition of $2\alpha/a^3$ =1can be satisfied. Therefore, the equations (4) and (5) are converted to Bakhshiev solvent polarity functions (Eq.8 and 9).

$$f_{BK}\left(\varepsilon,n\right)=\frac{2n^2+1}{n^2+2}\left[\frac{\varepsilon-1}{\varepsilon+2}-\frac{n^2-1}{n^2+2}\right] \quad (8)$$

$$g_{BK}\left(n\right)=\frac{3}{2}\left[\frac{n^4-1}{(n^2+2)^2}\right] \quad (9)$$

With approximation of parallel dipole moments of ground and excited states, we can write:

$$\mu_g = \left|\frac{m_2 - m_1}{2}\right| \left[\frac{hca^3}{2m_1}\right]^{1/2} \tag{10}$$

$$\mu_e = \left|\frac{m_2 + m_1}{2}\right| \left[\frac{hca^3}{2m_1}\right]^{1/2} \tag{11}$$

$$\mu_e = \frac{m_1 + m_2}{m_1 - m_2} \mu_g \left(m_1 \succ m_2\right) \tag{12}$$

Where *h* is Plank's constant and *c* is velocity of light in vacuum. In addition, $\mu_g$ and $\mu_e$ indicate ground and excited state's dipole moments, respectively. Onsager cavity radius (*a*) of pyridine compounds was also determined theoretically according to their optimized geometry.

### *2.4. Theoretical methods*

In this work, the molecular structures of selected samples were optimized by density functional theory (DFT) using M06-2X hybrid meta-functional and 6-31G (d, p) basis set [32-34]. By using these optimized structures (Fig. 1), time-dependent density functional theory (TDFT)was employed for investigation of molecular vertical excitations [35]. In addition, the molecular orbitals included in $\lambda_{\max}$ transition of these molecules are shown in Fig.1. These molecular orbitals are the highest occupied molecular orbital (HOMO) and the lowest unoccupied molecular orbital (LUMO).

It is useful to know that all of DFT calculations were performed by NWChem quantum chemistry program [36]. Furthermore, Onsager radii of the samples were determined by the same method [37]. All of obtained theoretical results for dipole moment values, the most probable excitation wavelengths, and related oscillator strengths can be found in Table 3. Along with these results, for precise investigation of solvent induced effects, molecular electrostatic potential (MEP) and solvent accessible surface (SAS) were observable in Fig. 2 and Fig. 3, respectively.

## 3. Result and discussion

### *3.1. The solvent effect on the absorption and fluorescence spectra*

In this section, spectroscopic technique as an applicable method is used for investigation of media polarity effects. In this case, the absorption and emission spectra of the pyridine parent molecules in various solvent media were recorded at room temperature according to Fig. 4-6. Moreover, for precise investigation of mentioned figures, the absorption spectra of samples are plotted in different solvent media, separately that they are available in supplementary data.

Pyridine compounds with different position of N-atoms and various active functional groups in their chemical structures indicate various active bands in the range of 270-370 nm (Table 4-6).Hence pyridine and C=N groups can have significant roles in molecular behavior.

The selected samples indicate two active absorption bands in UV region of electromagnetic spectrum. By changing the position of N-atoms in pyridine rings, the observable absorption bands are modified. In contrast to sample II and III, high energy band of sample I occur in the limited of solvents. As seen in Fig.4-6, similar behaviors are also observed in the emission characteristics of selected samples. In this case, the fluorescence spectra were recorded by excitation the samples at fixed wavelength (maximum absorption wavelength). According to DFT calculations, these behaviors can be related to transition between various molecular orbitals that for all of the samples $\pi \rightarrow \pi^*$ transitions are dominant (Fig.1). Moreover, the theoretical results from DFT calculation are accessible in Table 3.

In general, environment effects on the solvatochromism characteristics of materials are usually studied in the term of polarity parameter. According to Lippert equation, general solute-solvent interactions can be described in terms of the orientation polarizability parameter ($\Delta f$). Hence, for studying the solvent effects on the spectral characteristics of pyridine compounds, the maximum absorption and emission wavelengths are plotted as a function of orientation polarizability ($\Delta f$) of solvents. In this case, we focus on general solvent interactions effects on the spectral behavior of low and high-energy bands of pyridine compounds. The linear shown in Fig.7 and 8, help to the reader to recognize the blue and red shifts of used samples in different solvents with various polarity.

As can be seen in Fig. 7, in sample II and sample III, maximum absorption wavelengths tend to be shifted toward the long wavelength region by increasing orientation polarizability ($\Delta f$).In this case, similar behavior occurs in emission process. In sample I, by increasing the solvent polarity parameter ($\Delta f$), two active absorption bands shift toward the low wavelength region and negative solvatochromism process occur.

Moreover, the revealed differences between the absorption and emission of selected samples in various solvents media lead to phenomenon that is well known as Stokes shift. In real, fluorescence process occurs slower than the absorption process and at these circumstances; solvent molecules have enough time to reorient around to the solute molecules in the excited state. Therefore, emission process occurs at the relaxed state. In this case, the increasing of Stokes shifts ($\nu_a$-$\nu_b$) accompanied with increasing the polarity of organic solvents is due to reorientation of solvent molecules around to the solute molecules (Fig. 8). It should be noted that opposite behavior is observed in the first band of sample III.

A comparison among the experimental results indicates that the observable different spectral shifts is related to different position of N-atoms in pyridine ring of compounds and different active functional groups in their chemical structures. These differences can induce various solute-solvent interactions that lead to observation of various spectral behaviors.

Although above explanations can describe the general solvent effects qualitatively, they cannot describe completely the contribution of specific and nonspecific solute-solvent interaction's effects. For this reason in the next section, we will use the multi-parameter solvent polarity scales.

### *3.2. Correlation with multi-parameter solvent polarity scale*

In order to investigate the various solute-solvent interaction's contribution on the spectral characteristics of pyridine compounds, multi-parameter solvent polarity scales that are known as Kamlet- Abboud- Taft and Catalan formulation, were used. In the first step, all solvents were selected for multi-parameter analysis. Then according to the statistical factors ($R^2$ and significance of F-test) and visual inspection, the appropriate solvents were selected for obtaining the best results. Multiple linear analysis of absorption, emission and stokes shift data with multi-parameter polarity scales show the satisfactory correlation for selected collection of solvents. The obtained results are summarized in Table 7 and 8. For the better comparison of data in Table 7 and 8, we transformed them into contribution percentages of various solvent polarity parameters (Table 7 (b) and 8 (b)).

The results from the multiple linear analyses (Table 7) indicate that by transition to the excited state, solvent dipolarity/polarizability and solvent hydrogen bond acceptor abilities play significant role on the spectral shifts of high- and low energy bands of sample I, respectively. In similar analysis to the sample I, solvent specific interactions with high contribution have important effect on the observable absorption properties of low- and high energy bands of sample II. In comparison to the ground state, by excitation to the excited state, solvent hydrogen bond donor and solvent dipolarity/polarizability abilities play significant role on the photo-physical behavior of high- and low energy bands, respectively. In addition to these solvent polarity parameters, other polarity parameters with lower contribution play minor role on the photo-physical behavior of two active bands of sample II in the excited state. Therefore, absorption and fluorescence characteristics of low- and high energy bands are due to both specific and nonspecific interactions with different contributions.

In contrast to sample I and II, solvent hydrogen bond acceptor and solvent dipolarity/polarizability abilities have the same contribution in the absorption properties of high-energy band of sample III. By excitation to the excited state, the contribution of solvent dipolarity/polarizability ability is decreased and the contributions of solvent hydrogen bond donor and acceptor abilities are increased. The similar analysis for low-energy band indicates that in the ground state, solvent hydrogen bond acceptor ability and in the excited state, solvent dipolarity/polarizability ability have dominant contribution.

As discussed in previous section, the difference between the absorption and emission wavelengths leads to Stokes shift. Hence, investigation on the linear correlation between Stokes shift data and multi-parameter solvent polarity scales will give important information about the solvent polarity effects on the molecular reorientation. The experimental results (Table 7) indicate that in the most cases, the increment of dominant solvent polarity parameters increase stokes shifts of used samples. In this case, reorientation of solute molecules is increased in various solvent media.

Now, we exploit of Catalan multi-parameter solvent polarity scales for description of solvent effects. The advantage of this formulation in comparison to the Kamlet–Taft solvatochromic model is separation of nonspecific solvent effects into two dipolarity and polarizability terms. Therefore, in Eq. 1, the coefficient *c* is divided into *c* and *d* that they are describe the contribution of solvent dipolarity (SP) and polarizability (SdP) abilities, respectively.

According to the obtained experimental results (Table 8), in the most cases, there are good correlation between absorption, emission and stokes shift data with Catalan multi-parameter solvent scales. The data in parenthesis in Table 7 and 8 indicate the number of selected solvents in multi-parameter analysis.

In high-energy band of sample I, solvent dipolarity parameter has dominant role in its absorption characteristic. Moreover, the multi-linear analysis indicates that in the excited state, the correlation between Catalan solvent polarity parameters and first emission band of this sample is weak. In low-energy band of sample I, solvent acidity in the ground state and solvent basicity in the excited state as effective solvent polarity parameters play a significant role in the molecular photo-physical behavior. In sample II, solvent dipolarity have high contribution in the ground and excited states of two observable active bands. The similar solvent effect is also observed on the absorption characteristics of sample III. Furthermore, the analysis of solvent effects on the emission characteristics of two active bands of sample III reveals this fact that solvent acidity and solvent dipolarity with high contribution have significant effect on the excited state properties of low and high-energy bands, respectively. Moreover, similar analysis for stokes shifts data (Table 8) indicate that by increasing dominant solvent polarity parameters (except the high-energy band of sample III), the reorientation of solute molecules are increased in various solvent media.

In addition to the solvent effect on the spectral properties of used samples, it can effect on the stability of ground and excited states of solute molecules. Through the investigation on the stability of ground and excited states by changing each of solute-solvent contribution coefficient sign, it is clear that absorption is an instantaneous event and absorption spectroscopy give only information about the ground state of the molecules. Increasing the positive coefficients in Eq. (1) leads to stability of ground state. In contrast, fluorescence lifetime is usually longer than solvent relaxation time. Hence, fluorescence spectra illustrate the excited state of molecule. Therefore, increasing the negative coefficients in Eq. (1) increases the stability of excited state [38-39]. According to data in Table 7 and 8, in both selected models, dominant solvent polarity parameters lead to stability of ground and excited state of sample I. Dominant solvent polarity parameters also stabilize the excited state of low-energy band of sample II. Moreover, the similar behavior is observed in low-energy band of sample III.

In addition to the solvent effects on the spectral characteristics of pyridine compounds, they can alter the electronic structure and charge distribution properties of the solute molecules. For this reason, in the next section, the dipole moments of solute molecules are calculated and investigated in the ground and excited states.

### *3.3. Estimation of ground and excited state dipole moment*

For calculation of dipole moments of pyridine compounds, first solvent polarity functions, $f(\varepsilon,n)$ and $f(\varepsilon,n)+2g(n)$, were calculated (Table 2). Then the spectral shifts $\nu_a$-$\nu_f$ and $\nu_a$+$\nu_f$ of the selected sample were plotted as a function of solvent polarity functions $f(\varepsilon,n)$ and $f(\varepsilon,n)+2g(n)$, respectively, (Fig. 8). Hence, the points in Fig. 9 indicate the spectral shifts of samples in specific solvents with certain solvent polarity parameters. Moreover, according to the statistical factors ($R^2$), we deleted some solvents and selected the proper solvent collections. Finally, using the slopes of these lines and equations of (10) and (11) the ground and excited state dipole moments of samples were calculated. The obtained experimental results in various solvent media can be seen in Table 9.

The revealed experimental results indicate that the first excited state dipole moment values are higher than the ground state dipole moments in solvent media. On the other hand, dipole moments of the high-energy bands are smaller than the low-energy bands for three mentioned samples. The increase of excited state dipole moments of high and low-energy bands of sample I in solvent media with different polarity are about 3.55 and 3.77 Debye. The similar calculations indicate that these values are higher in sample II and III in comparison to sample I. The differences between ground and excited state dipole moments are about 6.83 and 6.34 Debye in high-energy band of sample II and sample III, respectively. These changes are also about 7.33 and 8.99 Debye for low-energy band of sample II and sample III, respectively. These results are in good agreement with DFT calculations. It is noticeable that DFT calculations have been performed in gas phase. Hence, dipole moments calculated by DFT method are usually different from experimental values. However, the trend of DFT data is in agreement with experimental ones. As it can be observed in Table 3, the differences between ground and excited state dipole moments ($\Delta\mu$) indicate that excited states have higher dipole moments in comparison with their ground states. In addition, DFT calculations predict higher $\Delta\mu$ values for lower energy bonds of calculated samples. The observable changes in dipole moment values of samples are highly sensitive to the possible resonance structures in various solvent media. In real, the various solute-solvent interactions can affect the electronic structure of solute molecules that the statistical weight for contribution of resonance structures depends highly on the molecular interactions. These resonance structures are obvious from HOMO and LUMO molecular orbital of these samples; see Fig. 1. As it can be seen from this figure, location of π bonds is different in HOMO and LUMO orbitals.

Moreover, the large differences between ground and excited state dipole moments increase the probability of charge transfer in solute molecules that are depend on the position and presence of active groups in the molecular chemical structures.

In this case, sample I with an electron-withdrawing group (COOH) in its terminal part tends to pull non-bonding electrons on the nitrogen atoms toward itself and leads to local intramolecular charge transfer. A comparison between dipole moment values of this sample with two other used samples reveals that increasing of conjugated length can lead to increment of dipole moments of sample II and III. On the other hand, the differences dipole moment values of sample II and III can be related to different position of nitrogen atoms in their pyridine rings.

Other results can be obtained by considering molecular electrostatic potential (MEP) and solvent accessible surface (SAS) of these molecules. MEP describes the regions of used molecules with positive and negative charges. According to Fig 2, the density of positive charges in sample I and II are more than sample III. Therefore, depend on the contribution of positive and negative charges on the solute molecules, the solute-solvent interactions can be modify. Under this condition, in contrast to positively charge regions, the negatively charged regions operate as a good electron donor agent in solvent media. Moreover, solvent accessible surface (SAS) values give useful information. As can be seen in Fig 3, the largest SAS value is related to sample II. This large interaction surface can increase the stability the structural form of sample II in comparison two others samples.

Therefore, solute-solvent interactions and induced resonance structures can be modified by presence of various active groups, position of N atoms, various contribution of negatively and positively charges on the solute molecules and solvent accessible surfaces while they have significant effects on dipole moment values.

## 4. Conclusions

The experimental results of spectroscopic and quantum chemistry methods reveal the interesting characteristic of pyridine compounds. The experimental results indicate that various solute-solvent interactions, position of atoms and active functional groups have profound effects on the interactional behavior of selected samples.

For precise investigation of specific and nonspecific solute-solvent interaction’s contribution on the photo-physical behaviors of samples, Kamlet-Abboud-Taft and Catalan models were employed, separately. According to the results, in most cases, there were good correlations between spectral data with Catalan multi-parameter solvent scales that it gives a possibility to separate non-specific solvent effects into dipolarity and polarizability terms. Furthermore, the dynamic behavior of pyridine samples as widely used compounds in pharmaceuticals was studied by stokes shifts results in various environments.

According to the results, dipole moment values are dependent on the solute-solvent interactions and induced resonance structures properties. In this case, presence of various active groups, position of N atoms, solvent accessible surfaces, and various contribution of negatively and positively charges on the solute molecules have significant effects on the dipole moment values. Moreover, the large differences between the ground and excited state dipole moments increase the probability of intramolecular charge transfer process by excitation.

Moreover, the majority of works are usually focus on the compounds with N atoms outside of aromatic rings while in this work, the effect of N atoms inside the aromatic rings and the effect of their position was investigated. On the other hand, these materials with pyridine rings can play important role in pharmaceuticals as an anti-cancer agent. Hence, investigation of the operation of these materials in various solvent environments can give useful information about their behaviors in various phenomena.

Therefore,, dipole moment values, interactional behavior, and recognizing environment polarity effects on the electronic structure of selected pyridine compounds, can give valuable information about how these samples can operate in various physical, chemical and biological phenomena. In other words, obtained results of operation of pyridine compounds in various solvent environments can be expanded to the biologically important environments with similar polarity characteristics.

**Acknowledgment:**

This work was supported by university of Tabriz.

## References

[1] S. Shimizu, N. Watanabe, T. Kataoka, T. Shoji, N. Abe, S. Morishita, H. Ichimura, Pyridine and Pyridine Derivatives, Wiley-VCH Verlag GmbH & Co. KGaA, Germany, 2000.

[2] M. A. Varfolomeev, M. A. Stolov, R. N. Nagrimanov, I. T. Rakipov, W. E. AcreeJr, M. H. Abraham, Analysis of solute-pyridine intermolecular interactions based on experimental

enthalpies of solution and enthalpies of solvation of solutes dissolved in pyridine, Thermochim Acta, 660 (2018) 11-17. https://doi.org/10.1016/j.tca.2017.12.016

[3] Y. K. Shi, B. Wang, X. L. Shi, Y.D. Zhao, B. Yu, H. M. Liu, Synthesis and biological evaluation of new steroidal pyridines as potential anti-prostate cancer agents, Eur. J. Med. Chem., 145 (2018) 11-22. 10.1016/j.ejmech.2017.12.094

[4] S. Prachayasittikul, R. Pingaew, A. Worachartcheewan, N. Sinthupoom, V. Prachayasittikul, S. Ruchirawat, V. Prachayasittikul, Roles of Pyridine and Pyrimidine Derivatives as Privileged Scaffolds in Anticancer Agents, Mini Rev. Med. Chem.,17 (2017) 869-901. 10.2174/1389557516666160923125801

[5] A. G. Amr, A. M. Mohamed, S. F. Mohamed, N. A. Abdel-Hafez, A. F. Hammam, Anticancer activities of some newly synthesized pyridine, pyrane, and pyrimidine derivatives, Bioorg Med. Chem., 14 (2006) 5481-5488. 10.1016/j.bmc.2006.04.045

[6] A. A. Altaf, A. Shahzad, Z. Gul, N. Rasool, A. Badshah, B. Lal, E. Khan, A Review on the Medical Importance of Pyridine Derivatives, JDDMC, 1 (2015)1-11. 10.11648/j.jddmc.20150101.11

[7] M. E. Castro, M. J. Percino, V. M. Chapela, M. Ceron, G. Soriano-Moro, J. Lopez-Cruz, F. J. Melendez, Int. J. Mol. Sci., 14 (2013) 4005-4029. https://doi.org/10.3390/ijms14024005

[8] K. L. Ameta, A. Dandia, Multicomponent Reactions Synthesis of Bioactive Heterocycles, CRC Press, Boca Raton, 2017.

[9] R. Ugo, Aspects of homogeneous catalysis, volume 5, D. Reidel Publishing Company, Boston, 1984.

[10] A. Hantzsch, Ueber die Synthese Pyridineartiger Verbindungen aus Actessigather und Aldehydammoniak, Justus Liebigs Ann. Chem., 215 (1882) 72. https://doi.org/10.1002/jlac.18822150102

[11] T. Usuki, T. Sugimura, A. Komatsu, Y. Koseki, Biomimetic Chichibabin Pyridine Synthesis of the COPD Biomarkers and Elastin Cross-Linkers isodesmosine and Desmosine, Org. Lett., 16 (2014) 1672-1675. 10.1021/ol500333t

[12] C. Reichardat, Solvents and solvent effects in Organic chemistry, third Edition, Wiley-VCH Verlag GmbH& Co. KGaA, Weinheim, 2003.

[13] M. J. Kamlet, R. W. Taft, Linear solvation energy relationships. Part 3. Some reinterpretations of solvent effects based on correlations with solvent effects based on correlations with solvent π* and α values, J. Chem. Soc., Perkin Trans., 2 (1979) 349-356. 10.1039/P29790000349

[14] M. J. Kamlet, R. W. Taft, The solvatochromic comparison method. I. The beta-scale of solvent hydrogen-bond acceptor (HBA) basicities, J. Am. Chem. Soc., 98 (1976) 377-383. 10.1021/ja00418a009

[15]J. L. Abboud, M. J. Kamlet and R. W. Taft, Regarding a generalized scale of solvent polarities, J. Am. Chem. Soc., 99 (1977). 8325-8327. 10.1021/ja00467a039

[16] J. Catalan, Toward a Generalized Treatment of the Solvent Effect Based on Four Empirical Scales: Dipolarity (SdP, a New Scale), Polarizability (SP), Acidity (SA), and Basicity (SB) of Medium, J. Phys. Chem. B, 113 (2009) 5951-5960.10.1021/jp8095727

[17] G. Wypych, Handbook of Solvents, second Edition, Volume 1. Properties, ChemTec, Toronto, 2014.

[18]J-Y. Wu, F-Y. Cheng, M-H. Chiang, J. Solid State Chem., 242 (2016) 8-13. https://doi.org/10.1016/j.jssc.2016.06.021

[19]N. Rad-Yousefnia, B. Shaabani, M. Kubicki, M. S. Zakerhamidi, A. M. Grzeskiewicz, 2D holodirected lead (II) halide coordination polymers based on rigid N,N'-bis (4-pyridlmethylidyne) phenylene-1, 4-diamine ligand: Syntheses, crystal structure, NBO studies and luminescence properties, Polyhedron, 129 (2017) 38-45. https://doi.org/10.1016/j.poly.2017.03.022

[20] Q-F. Hou, L. Ye, S-M. Jiang, Acta Cryst., Section E, 63 (2007) o939-o940. https://doi.org/10.1107/S1600536807002978

[21] Q. Wang, D-Q. Wang, Y-Y. Sun, N, N'-Bis (4-pyridylmethylene) benzene-1,4-diamine monohydrate, Acta Cryst., Section E: Structure Reports Online, 63 (2007) o4665-o4665. 10.1107/S1600536807056711

[22] K. Ha, A centrosymmetric monoclinic polymorph of $N^1$, $N^4$-bis(pyridine-3-yl-methylidene) benzene- 1, 4-diamine, Acta Cryst., Section E: Structure Reports Online, 67 (2011) o2250-o2250. 10.1107/S1600536811030789

[23] H-N, Kim, H-K. Lee, S-W. Lee, A Novel Linking Schiff-Base Type Ligand (L: py-CH=N-$C_6H_4$-N=CH-py) and Its Zinc Coordination Polymers: Preparation of L, 2-Pyridine-3-yl-1H-benzoimidazol, trans-[Zn $(H_2O)_4L_2].(NO_3)_2$, $[Zn(NO_3)(H_2O)_2(L)].(NO_3).(H_2O)_2$, and [Zn(L)(OBC)(H2O)] ( OBC=4,4'-Oxybis(benzoate)), Bull.Korean Chem. Soc., 26 (2005) 892-898. 10.5012/bkcs.2005.26.6.892

[24] W. Liptay, Electrochromism and solvatochromism, Angew. Chem. interant. Edit., 8 (1969) 177-188. https://doi.org/10.1002/anie.196901771

[25] J.R. Lombardi, Dipole Moment of the Lowest Singlet π*←π States in Phenol and Aniline by the Optical Stark Effect, J. Chem. Phys., 50 (1969) 3780-3783. https://doi.org/10.1063/1.1671626

[26] V. I. Minkin, O. A. Osipov, Y. A. Zhdanov, Dipole moments in organic chemistry, Plenum Press, New York-London, 1970.

[27] M.P. De Haas, Photon-induced molecular charge separation studied by nanosecond time-resolved microwave conductivity, J. M. Warman, Chem. Phys., 73 (1982) 35-53. https://doi.org/10.1016/03010104(82)85148-3

[28] M. Khadem Sadigh, M.S. Zakerhamidi, S.M. Seyed Ahmadian, M. Johari-Ahar, L. Zare Haghighi, Environment effect on spectral and charge distribution characteristics of some drugs of folate derivatives, J. Spectrochim Acta A Mol Biomol Spectrosc., 171 (2017) 10-17.10.1016/j.saa.2016.07.034

[29] M. Khadem Sadigh, M.S. Zakerhamidi, A.N. Shamkhali, E. Babaei, Photo-physical behaviors of various active forms of curcumin in polar and low polar environments, J. Photochim.Photobiol A., 348 (2017) 188-198. https://doi.org/10.1016/j.jphotochem.2017.08.050

[30] A. Kawski, Progress in Photochemistry and Photophysics, in: J. F. Rabek (Ed), Volum 5, CRC Press Boca Raton, Boston, 1992, pp.1-47.

[31] A. Kawski, On the Estimation of Excited- State Dipole moments from Solvatochromic Shifts of Absorption and Fluorescence Spectra, Z. Naturforsch., 57a (2002) 255-262. · 10.1515/zna-2002-0509

[32] Y. Zhao and D. G. Truhlar, Comparative DFT Study of van der Waals Complexes: Rare-Gas Dimers, Alkaline-Earth Dimers, Zinc Dimer, and Zinc-Rare-Gas Dimers, J. Phys. Chem A, 110 (2006) 5121-5129.10.1021/jp060231d

[33] M. M. Francl, W. J. Pietro, W. J. Hehre, J. S. Binkley, M. S. Gordon, D. J. Defrees, J. A. Pople, Self-consistent molecular orbital methods, XXIII. A polarization-type basis set for second-row elements, J. Chem. Phys., 77 (1982) 3654. https://doi.org/10.1063/1.444267

[34] G. A. Petersson, T. G. Tensfeldt, J. A. Montgomery Jr., A complete basis set model chemistry. III. The complete basis set- quadratic configuration interaction family of methods, J. Chem. Phys., 94 (1991) 6091-6101. https://doi.org/10.1063/1.460448

[35] F. Furche, R. Ahlrichs, Adiabatic time-dependent density functional methods for excited state properties, J. Chem. Phys, 117 (2002) 7433-7447. https://doi.org/10.1063/1.1508368

[36] M. Valiev, E.J. Bylaska, N. Govind, K. Kowalski, T.P. Straatsma, H.J.J. van Dam, D. Wang, J. Nieplocha, E. Apra, T.L. Windus, W.A. de Jong, NWChem: A comprehensive and scalable open-source solution for large scale molecular simulations, Comput Phys Commun, 181 (2010) 1477-1489. https://doi.org/10.1016/j.cpc.2010.04.018

[37] L. Onsager, Electronic Moments of Molecules in Liquids, J. Am. Chem. Soc., 58 (1936) 1486-1493. 10.1021/ja01299a050

[38] J. R. Lakowicz, Principles of fluorescence spectroscopy, Third Edition, Springer, USA, 2006.

[39] M. S. Zakerhamidi, K. Nejati, Sh. Golghasemi Sorkhabi, M. Saati, Substituent and solvent effects on the spectroscopic properties and dipole moments of hydroxyl benzaldehyde azo dye and

related Schiff bases, J. Mol. Liq., 180 (2013) 225-234. https://doi.org/10.1016/j.molliq.2013.01.021

## Figure captions:

**Fig. 1.** The calculated optimized structures of a) Sample I, b) sample II, and c) sample III and their involved HOMO and LOMO molecular orbital in the most probable vertical excitation by TDFDT method.

**Fig. 2.** MEP for optimized structures of a) sample I, b) Sample II, and c) sample III.

**Fig. 3.** SAS for optimized structures of a) sample I, b) sample II, and c) sample III.

**Fig.4.**a) Absorption and b) fluorescence spectral of sample I.

**Fig.5.** a) Absorption and b, c) fluorescence spectral of sample II.

**Fig.6.**a) Absorption and b, c) fluorescence spectral of sample III.

**Fig.7.** Variation of a) maximum absorption, b) emission wavelengths and c) stokes shift of used samples as a function of orientation polarizability parameter ($\Delta f$).

**Fig.8.** Variation of stokes shifts of a) sample I, b) sample II, and c) sample III as a function of orientation polarizability parameter ($\Delta f$).

**Fig. 9.** The variation of $\nu_a$-$\nu_f$ with $f(\varepsilon,n)$ and $\nu_a+\nu_f$ with $f(\varepsilon,n)+2g(n)$ for a) sample I, b)sample II and c)sample III.

## List of Tables:

**Table 1**. Molecular name, molecular structure and molecular weight of used samples.

**Table 2.** Solvent polarity parameters, physical properties and polarity functions of employed solvents.

**Table 3**. TDDFT results for pyridine samples with dipole moments (Δμ) of the most probable excitations, their wavelengths $\lambda_{max}$, oscillator strengths (*f*), and involved molecular orbitals.

**Table 4.** Absorbance and fluorescence data of sample I in various solvents.

**Table 5.** Absorbance and fluorescence data of II in various solvents.

**Table 6.** Absorbance and fluorescence data of III in various solvents.

**Table 7.** a) Regression fit to Kamlet-Abboud-Taft multi-parameter solvent polarity scales for absorbance, fluorescence and stokes shift of used samples b) Percentage contribution of various solute-solvent interactions.

**Table 8.** a) Regression fit to Catalan multi-parameter solvent polarity scales for absorbance, fluorescence and stokes shift of used samples b) Percentage contribution of various solute-solvent interactions.

**Table 9.** Dipole moments and essential parameters for measuring them.

| Molecular structure and Molecular name | Molecular weight (g/mol) |
|---|---|
| 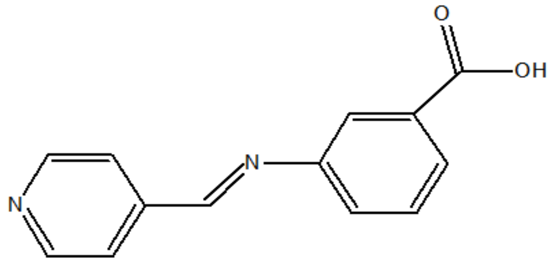<br>(E)-3-(pyridin-4-ylmethyleneamino)benzoic acid<br>(Sample I) | 226.23 |
| 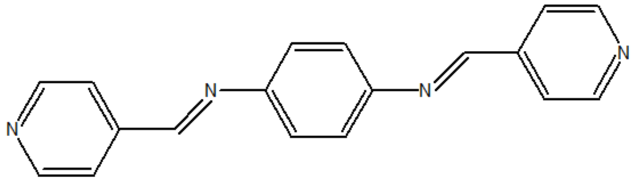<br>(N$^{1}$E,N$^{4}$E)-N$^{1}$,N$^{4}$-bis(pyridin-4-ylmethylene)benzene-1,4-diamine<br>(Sample II) | 286.33 |
| 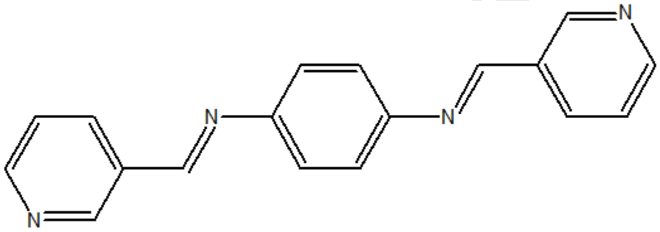<br>(N$^{1}$E,N$^{4}$E)-N$^{1}$,N$^{4}$-bis(pyridin-3-ylmethylene)benzene-1,4-diamine<br>(Sample III) | 286.33 |

Table 1. Molecular name, molecular structure and molecular weight of used samples.

Table 2. Solvent polarity parameters, physical properties and polarity functions of employed solvents.

| solvent | $\varepsilon_r$ | n | $\alpha$ | $\beta$ | $\pi^*$ | SP | SdP | SA | SB | $\Delta f$ | $f(\varepsilon,n)+2g(n)$ | $f(\varepsilon,n)$ |
|---|---|---|---|---|---|---|---|---|---|---|---|---|
| Water | 78.40 | 1.333 | 1.17 | 0.47 | 1.09 | 0.681 | 0.997 | 1.062 | 0.025 | 0.319 | 1.364 | 0.912 |
| DMSO | 46.68 | 1.479 | 0.00 | 0.76 | 1.00 | 0.830 | 1.000 | 0.072 | 0.647 | 0.263 | 1.488 | 0.84 |
| DMF | 38.00 | 1.430 | 0.00 | 0.69 | 0.88 | 0.759 | 0.977 | 0.031 | 0.613 | 0.275 | 1.422 | 0.838 |
| Ethylene glycol | 37.00 | 1.430 | 0.90 | 0.52 | 0.92 | 0.777 | 0.910 | 0.717 | 0.534 | 0.274 | 1.419 | 0.836 |
| Methanol | 32.70 | 1.329 | 0.98 | 0.66 | 0.60 | 0.608 | 0.904 | 0.605 | 0.545 | 0.308 | 1.302 | 0.854 |
| Ethanol | 24.50 | 1.361 | 0.86 | 0.75 | 0.54 | 0.633 | 0.783 | 0.400 | 0.658 | 0.288 | 1.304 | 0.812 |
| Acetone | 21.01 | 1.359 | 0.08 | 0.48 | 0.62 | 0.651 | 0.907 | 0.000 | 0.475 | 0.284 | 1.281 | 0.792 |
| 2-propanol | 19.92 | 1.377 | 0.76 | 0.84 | 0.48 | 0.633 | 0.808 | 0.283 | 0.830 | 0.276 | 1.291 | 0.778 |
| 1-Butanol | 17.50 | 1.399 | 0.84 | 0.84 | 0.47 | 0.674 | 0.655 | 0.341 | 0.809 | 0.263 | 1.292 | 0.75 |
| 1-Hexanol | 13.00 | 1.418 | 0.67 | 0.94 | 0.40 | 0.698 | 0.552 | 0.315 | 0.879 | 0.243 | 1.253 | 0.686 |
| 1-Heptanol | 11.30 | 1.424 | 0.64 | 0.96 | 0.39 | 0.706 | 0.499 | 0.302 | 0.912 | 0.233 | 1.227 | 0.652 |
| Dichloromethane | 8.93 | 1.424 | 0.13 | 0.10 | 0.73 | 0.761 | 0.769 | 0.040 | 0.178 | 0.217 | 1.165 | 0.59 |
| 1-Decanol | 8.00 | 1.437 | 0.70 | 0.85 | 0.45 | 0.722 | 0.383 | 0.259 | 0.912 | 0.204 | 1.145 | 0.552 |
| Diethyl ether | 4.34 | 1.349 | 0.00 | 0.47 | 0.24 | 0.617 | 0.385 | 0.000 | 0.562 | 0.168 | 0.854 | 0.379 |
| 1,4-Dioxane | 2.22 | 1.420 | 0.00 | 0.37 | 0.49 | 0.737 | 0.312 | 0.000 | 0.444 | 0.022 | 0.615 | 0.045 |
| Cyclohexane | 2.02 | 1.426 | 0.00 | 0.00 | 0.00 | 0.683 | 0.000 | 0.000 | 0.073 | -0.001 | 0.574 | -0.003 |

Table 3. TDDFT results for pyridine samples with dipole moments ($\Delta\mu$) of the most probable excitations, their wavelengths $\lambda_{max}$, oscillator strengths (*f*), and involved molecular orbitals.

| Molecular Name | $\Delta\mu$ (Debye) | $\lambda_{max}$(nm) | *f* | Excitation Type |
|---|---|---|---|---|
| Sample I | | | | |
| Low energy band | 1.220 | 308.69 | 0.1489 | $\pi \rightarrow \pi^*$ |
| High energy band | 1.780 | 249.41 | 0.3895 | $\pi \rightarrow \pi^*$ |
| Sample II | | | | |
| Low energy band | 2.668 | 308.00 | 0.6344 | $\pi \rightarrow \pi^*$ |
| High energy band | 2.663 | 262.22 | 0.8253 | $\pi \rightarrow \pi^*$ |
| Sample III | | | | |
| Low energy band | 2.84 | 336.38 | 0.7305 | $\pi \rightarrow \pi^*$ |
| High energy band | 2.17 | 270.00 | 0.5313 | $\pi \rightarrow \pi^*$ |

Table 4. Absorbance and fluorescence data of sample I in various solvents.

| solvent | (1) | | (2) | |
|---|---|---|---|---|
| | $\lambda_{Abs}$(nm) | $\lambda_{Flu}$(nm) | $\lambda_{Abs}$(nm) | $\lambda_{Flu}$(nm) |
| | | **Sample I** | | |
| Water | ----- | ----- | 292 | 408 |
| DMSO | ----- | ----- | 329 | 411 |
| DMF | ----- | ----- | 327 | 406 |
| Ethylene glycol | ----- | ----- | 322 | 415 |
| Methanol | ----- | ----- | 322 | 415 |
| Ethanol | 273 | 334 | 324 | 413 |
| Acetone | ---- | ----- | ---- | ---- |
| 2-propanol | 265 | 316 | 324 | 419 |
| 1-Butanol | 267 | 311 | 324 | 415 |
| 1-Hexanol | 273 | 350 | 323 | 415 |
| 1-Heptanol | 272 | 307 | 324 | 415 |
| Dichloromethane | ---- | ---- | 323 | 403 |
| 1-Decanol | 268 | 308 | 328 | 415 |
| Diethyl ether | ---- | ---- | 324 | 409 |
| 1,4-Dioxane | ---- | ---- | 324 | 396 |
| Cyclohexane | ---- | ---- | ---- | ---- |

Table 5. Absorbance and fluorescence data of sample II in various solvents.

| solvent | (1) | | (2) | |
|---|---|---|---|---|
| | $\lambda_{Abs}$(nm) | $\lambda_{Flu}$(nm) | $\lambda_{Abs}$(nm) | $\lambda_{Flu}$(nm) |
| | **Sample II** | | | |
| Water | ---- | ---- | 355 | 453 |
| DMSO | 277 | 335 | 366 | 440 |
| DMF | 282 | 337 | 363 | 415 |
| Ethylene glycol | 278 | 355 | 369 | 465 |
| Methanol | 277 | 307 | 363 | 433 |
| Ethanol | 274 | 318 | 363 | 417 |
| Acetone | ---- | ---- | 360 | 430 |
| 2-propanol | 278 | 314 | 364 | 411 |
| 1-Butanol | 281 | 311 | 364 | 436 |
| 1-Hexanol | ---- | ---- | 366 | 412 |
| 1-Heptanol | ---- | ---- | 366 | 434 |
| Dichloromethane | 276 | 330 | 360 | 438 |
| 1-Decanol | 280 | 305 | 366 | 429 |
| Diethyl ether | ----- | ---- | 359 | 427 |
| 1,4-Dioxane | ----- | ---- | 360 | 411 |
| Cyclohexane | 272 | 329 | 361 | 404 |

Table 6. Absorbance and fluorescence data of sample III in various solvents.

| solvent | (1) | | (2) | |
|---|---|---|---|---|
| | $\lambda_{Abs}$(nm) | $\lambda_{Flu}$(nm) | $\lambda_{Abs}$(nm) | $\lambda_{Flu}$(nm) |
| | **Sample III** | | | |
| Water | ---- | ---- | 348 | 419 |
| DMSO | 283 | 330 | 361 | 438 |
| DMF | 286 | 300 | 359 | 441 |
| Ethylene glycol | 280 | 310 | 360 | 440 |
| Methanol | 274 | 308 | 354 | 411 |
| Ethanol | 274 | 316 | 357 | 420 |
| Acetone | ---- | ---- | 357 | 429 |
| 2-propanol | 277 | 315 | 358 | 414 |
| 1-Butanol | 279 | 310 | 359 | 411 |
| 1-Hexanol | ---- | ---- | 360 | 412 |
| 1-Heptanol | ---- | ---- | 361 | 412 |
| Dichloromethane | 274 | 321 | 358 | 435 |
| 1-Decanol | 277 | 305 | 360 | 427 |
| Diethyl ether | ---- | ----- | 358 | 426 |
| 1,4-Dioxane | ---- | ----- | 358 | 419 |
| Cyclohexane | 268 | 322 | 353 | 410 |

Table 7. a) Regression fit to Kamlet-Abboud-Taft multi-parameter solvent polarity scales for absorbance, fluorescence and stokes shift ofused samples b)Percentage contribution of various solute-solvent interactions.

| Multi-parameter scale | $\nu_0$(10$^3$cm$^{-1}$) | a(10$^3$cm$^{-1}$) | b(10$^3$cm$^{-1}$) | c(10$^3$cm$^{-1}$) | R$^2$ |
|---|---|---|---|---|---|
| **Sample I** | | | | | |
| Absorbance | | | | | |
| High energy band | 25.967±9.262 | -1.574±1.752 | 4.202±6.132 | 19.692±9.714 | 0.97 (5) |
| Low energy band | 29.682±0.900 | 1.821±0.451 | -1.386±0.805 | 2.119±0.812 | 0.75 (12) |
| Fluorescence | | | | | |
| High energy band | 76.589±43.249 | 4.119±8.320 | -24.824±29.141 | -57.752±43.281 | 0.89 (5) |
| Low energy band | 24.700±0.175 | -0.226±0.095 | -0.692±0.174 | 0.300±0.153 | 0.84 (12) |
| Stokes shift | | | | | |
| High energy band | -32.954±12.664 | -2.322±2.436 | 20.468±8.533 | 48.895±12.674 | 0.98 (5) |
| Low energy band | 6.052±0.313 | 0.912±0.207 | 0.125±0.338 | -0.151±0.322 | 0.76 (13) |
| **Sample II** | | | | | |
| Absorbance | | | | | |
| High energy band | 36.758±0.264 | 0.511±0.328 | -1.160±0.426 | -0.607±0.377 | 0.72 (9) |
| Low energy band | 27.740±0.104 | 0.255±0.094 | -0.776±0.134 | 0.335±0.126 | 0.79 (14) |
| Fluorescence | | | | | |
| High energy band | 30.500±0.514 | 2.230±0.662 | 0.390±0.915 | -0.997±0.87 | 0.87 (9) |
| Low energy band | 24.840±0.457 | -0.615±0.438 | 0.704±0.627 | -2.631±0.570 | 0.75 (13) |
| Stokes shift | | | | | |
| High energy band | 0.781±1.929 | 1.080±0.925 | -1.751±1.334 | 7.040±1.796 | 0.83 (9) |
| Low energy band | 3.064±0.463 | 1.012±0.398 | -1.231±0.581 | 2.230±0.538 | 0.71 (15) |
| **Sample III** | | | | | |
| Absorbance | | | | | |
| High energy band | 37.375±0.274 | 0.594±0.285 | -1.314±0.413 | -1.328±0.373 | 0.86 (10) |
| Low energy band | 28.195±0.114 | 0.495±0.107 | -0.869±0.158 | 0.167±0.142 | 0.76 (15) |

| | | | | | |
|---|---|---|---|---|---|
| Fluorescence | | | | | |
| High energy band | 31.089±0.376 | -2.185±0.687 | 3.386±0.799 | -0.067±0.693 | 0.89 (7) |
| Low energy band | 24.211±0.246 | 0.980±0.229 | -0.260±0.339 | -1.369±0.305 | 0.76 (15) |
| Stokes shift | | | | | |
| High energy band | 6.613±0.64 | 1.693±0.803 | -3.588±1.042 | -2.489±0.923 | 0.83(9) |
| Low energy band | 3.973±0.238 | -0.409±0.213 | -0.700±0.319 | 1.632±0.285 | 0.77 (16) |

a)

| Multi-parameter scale | $P_\alpha$(%) | $P_\beta$(%) | $P_{\pi^*}$(%) |
|---|---|---|---|
| **Sample I** | | | |
| Absorbance | | | |
| High energy band | 6 | 17 | 77 |
| Low energy band | 34 | 26 | 40 |
| Fluorescence | | | |
| High energy band | 5 | 29 | 66 |
| Low energy band | 18 | 75 | 25 |
| Stokes shift | | | |
| High energy band | 3 | 29 | 68 |
| Low energy band | 77 | 10 | 13 |
| **Sample II** | | | |
| Absorbance | | | |
| High energy band | 22 | 51 | 27 |
| Low energy band | 19 | 57 | 24 |
| Fluorescence | | | |

| | | | |
|---|---|---|---|
| High energy band | 62 | 11 | 27 |
| Low energy band | 15 | 18 | 67 |
| Stokes shift | | | |
| High energy band | 11 | 18 | 71 |
| Low energy band | 23 | 27 | 50 |
| **SampleIII** | | | |
| Absorbance | | | |
| High energy band | 18 | 41 | 41 |
| Low energy band | 32 | 57 | 11 |
| Fluorescence | | | |
| High energy band | 39 | 60 | 1 |
| Low energy band | 38 | 10 | 52 |
| Stokes shift | | | |
| High energy band | 22 | 46 | 32 |
| Low energy band | 15 | 26 | 59 |

b)

Table 8. a) Regression fit to Catalan multi-parameter solvent polarity scales for absorbance, fluorescence and stokes shift of used samples b) Percentage contribution of various solute-solvent interactions.

| Multi-parameter scale | $\nu_0$(10$^3$cm$^{-1}$) | a(10$^3$cm$^{-1}$) | b(10$^3$cm$^{-1}$) | c(10$^3$cm$^{-1}$) | d(10$^3$cm$^{-1}$) | $R^2$ |
|---|---|---|---|---|---|---|
| **Sample I** | | | | | | |
| Absorbance | | | | | | |
| High energy band | -3.583±62.044 | 79.613±105.378 | 16.250±19.816 | -29.885±25.141 | -16.539±19.198 | 0.77 (6) |
| Low energy band | 32.621±1.690 | -0.836±2.285 | -0.628±0.684 | 1.989±0.547 | -1.884±0.564 | 0.81 (14) |
| Fluorescence | | | | | | |
| High energy band | 132.099±376.125 | -149.291±638.817 | -29.570±120.130 | 9.041±152.412 | 18.682±116.381 | 0.27 (6) |
| Low energy band | 24.813±0.601 | 1.154±0.813 | -0.545±0.243 | -0.522±0.194 | -1.214±0.200 | 0.84 (14) |
| Stokes shift | | | | | | |
| High energy band | -135.683±314.080 | 228.904±533.439 | 45.821±100.314 | -38.927±127.270 | -35.221±97.138 | 0.31 (6) |
| Low energy band | 7.807±1.712 | -1.991±2.316 | -0.083±0.693 | 2.512±0.554 | -0.670±0.571 | 0.81 (14) |
| **Sample II** | | | | | | |
| Absorbance | | | | | | |
| High energy band | 38.860±1.228 | -2.896±1.695 | -0.399±0.374 | 0.379±0.470 | -1.141±0.391 | 0.78 (9) |
| Low energy band | 29.271±0.513 | -1.886±0.723 | 0.106±0.169 | -0.171±0.164 | -0.729±0.155 | 0.71 (16) |
| Fluorescence | | | | | | |
| High energy band | -2.513±4.171 | 12.524±5.820 | 0.666±1.406 | 1.765±1.758 | -3.790±1.488 | 0.74 (10) |
| Low energy band | 30.963±2.067 | -9.232±2.847 | -0.339±0.622 | -2.475±0.652 | -0.070±0.520 | 0.77 (14) |
| Stokes shift | | | | | | |
| High energy band | -2.513±4.171 | 12.524±5.820 | 0.666±1.406 | 1.765±1.758 | -3.790±1.488 | 0.73 (9) |
| Low energy band | -1.914±2.019 | 7.618±2.782 | 0.450±0.608 | 2.348±0.637 | -0.647±0.508 | 0.78 (14) |
| **Sample III** | | | | | | |

| | | | | | | |
|---|---|---|---|---|---|---|
| Absorbance | | | | | | |
| High energy band | 40.465±1.241 | -4.291±1.731 | -1.017±0.418 | 0.407±0.523 | -1.243±0.443 | 0.87 (10) |
| Low energy band | 29.484±0.317 | -1.698±0.447 | -0.025±0.104 | 0.308±0.101 | -0.698±0.096 | 0.89 (16) |
| Fluorescence | | | | | | |
| High energy band | 31.907±1.990 | -0.847±2.780 | -1.331±0.734 | 2.500±0.944 | 1.029±0.712 | 0.78 (9) |
| Low energy band | 28.655±1.190 | -6.306±1.633 | -1.206±0.356 | 0.508±0.356 | 0.273±0.327 | 0.78 (15) |
| Stokes shift | | | | | | |
| High energy band | 8.578±1.913 | -3.569±2.671 | -2.619±0.907 | -2.619±0.907 | -2.218±0.684 | 0.87 (9) |
| Low energy band | 2.544±1.028 | 2.354±1.456 | 1.425±0.358 | -0.592±0.330 | -1.316±0.330 | 0.79 (15) |

a)

| Multi-parameter scale | $P_{SP}$(%) | $P_{SdP}$(%) | $P_{SA}$(%) | $P_{SB}$(%) |
|---|---|---|---|---|
| **Sample I** | | | | |
| Absorbance | | | | |
| High energy band | 56 | 11 | 21 | 12 |
| Low energy band | 16 | 12 | 37 | 35 |
| Fluorescence | | | | |
| High energy band | 72 | 14 | 4 | 9 |
| Low energy band | 34 | 16 | 15 | 35 |
| Stokes shift | | | | |
| High energy band | 66 | 13 | 11 | 10 |
| Low energy band | 38 | 1 | 48 | 13 |
| **Sample II** | | | | |
| Absorbance | | | | |
| High energy band | 60 | 8 | 8 | 24 |

| | | | | |
|---|---|---|---|---|
| Low energy band | 65 | 4 | 6 | 25 |
| Fluorescence | | | | |
| High energy band | 72 | 5 | 8 | 15 |
| Low energy band | 76 | 3 | 20 | 1 |
| Stokes shift | | | | |
| High energy band | 67 | 4 | 9 | 20 |
| Low energy band | 69 | 4 | 21 | 6 |
| **Sample III** | | | | |
| Absorbance | | | | |
| High energy band | 62 | 14 | 6 | 18 |
| Low energy band | 62 | 1 | 11 | 26 |
| Fluorescence | | | | |
| High energy band | 15 | 23 | 44 | 18 |
| Low energy band | 76 | 15 | 6 | 3 |
| Stokes shift | | | | |
| High energy band | 39 | 8 | 29 | 24 |
| Low energy band | 41 | 25 | 11 | 23 |

b)

Table 9. Dipole moments and essential parameters for measuring them.

| Sample's name | $m_1$ | $m_2$ | Radius $(A^\circ)$ | $\mu_g$(D) | $\mu_e$(D) | $\Delta\mu$ |
|---|---|---|---|---|---|---|
| **Sample I** | | | | | | |
| High energy band | 7391.7 | 2859 | 5.04 | 2.81 | 6.36 | 3.55 |
| Low energy band | 1591.2 | 1410.5 | 5.04 | 0.24 | 4.01 | 3.77 |
| **Sample II** | | | | | | |
| High energy band | 3338.9 | 9748.3 | 5.40 | 6.56 | 13.39 | 6.83 |
| Low energy band | 12865 | 7021.4 | 5.40 | 3.04 | 10.37 | 7.33 |
| **Sample III** | | | | | | |
| High energy band | 3009.4 | 9704.2 | 5.32 | 7.06 | 13.40 | 6.34 |
| Low energy band | 9060.8 | 7393.2 | 5.32 | 1.01 | 10.00 | 8.99 |

Research Highlights

> Media polarity has main role on the photo-physical behavior of pyridine compounds.

> Solute molecules with various positions of N atoms operate differently in solvents.

> Kamlet-Abboud-Taft and Catalan models are useful for studying molecular interactions.

> During the excitation process, samples tend to form a polar structure.

> The results can be expanded to the biological media with similar polarity features.

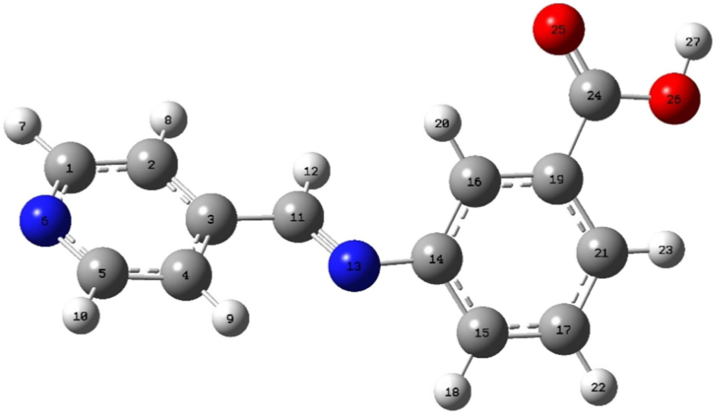

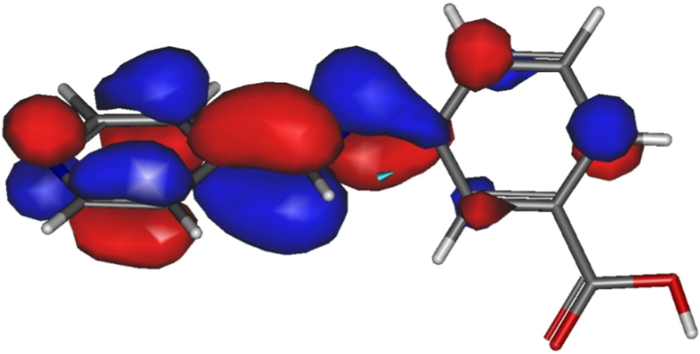

LUMO

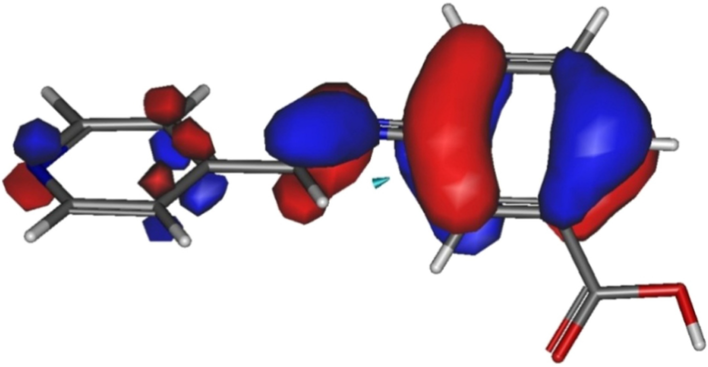

HOMO

a)

Figure 1a

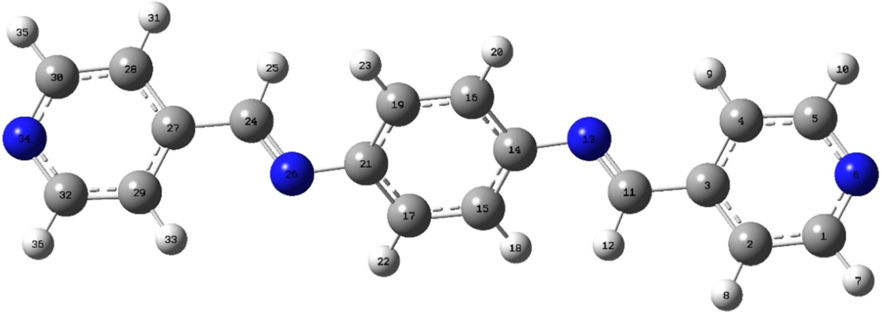

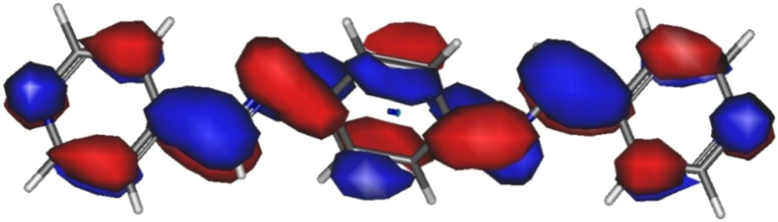

LUMO

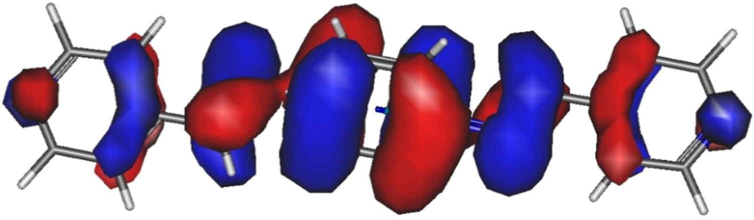

HOMO

b)

Figure 1b

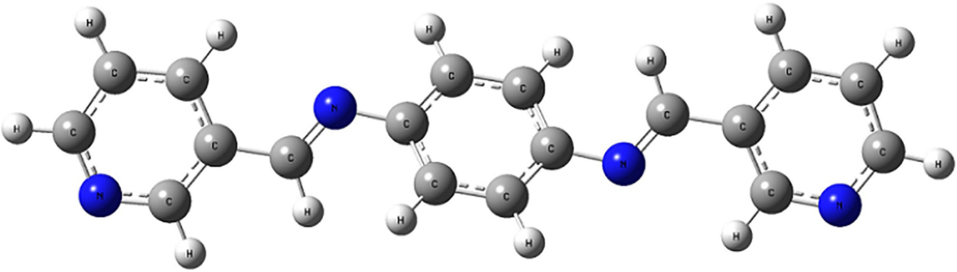

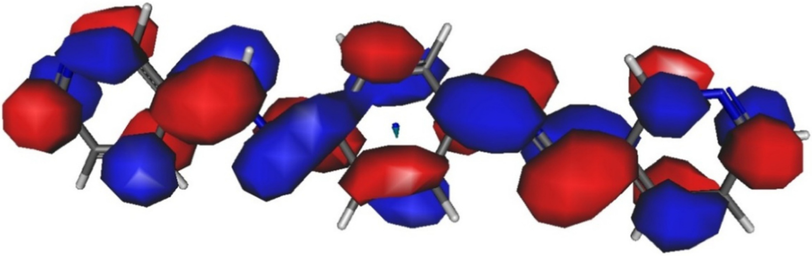

LUMO

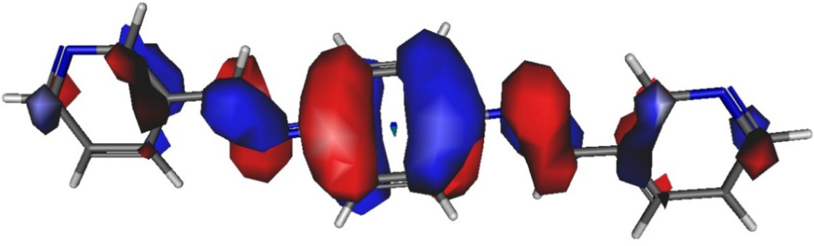

HOMO

c)

Figure 1c

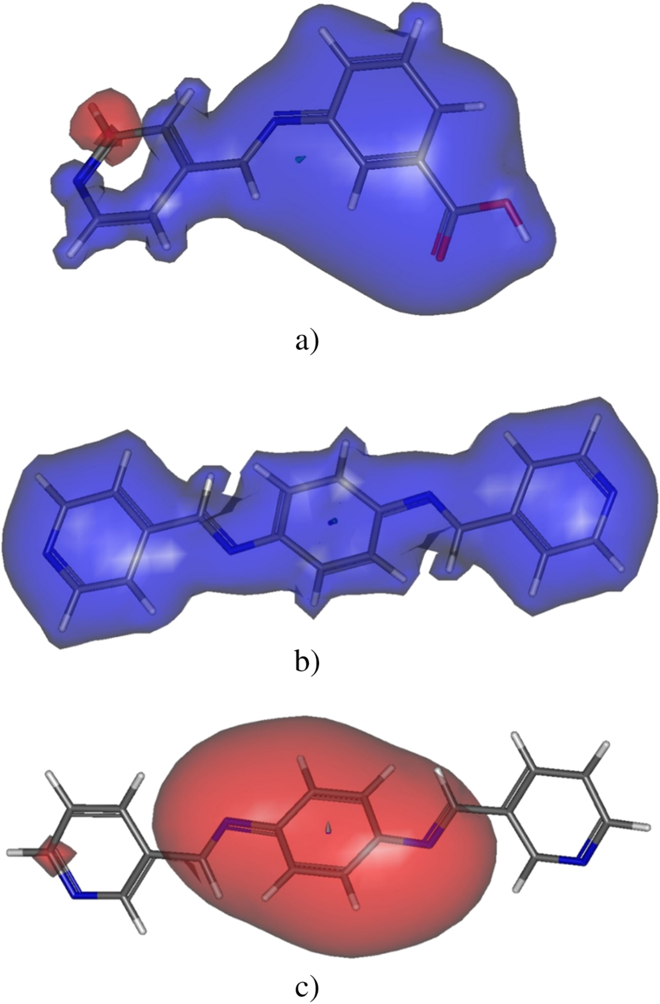

Figure 2

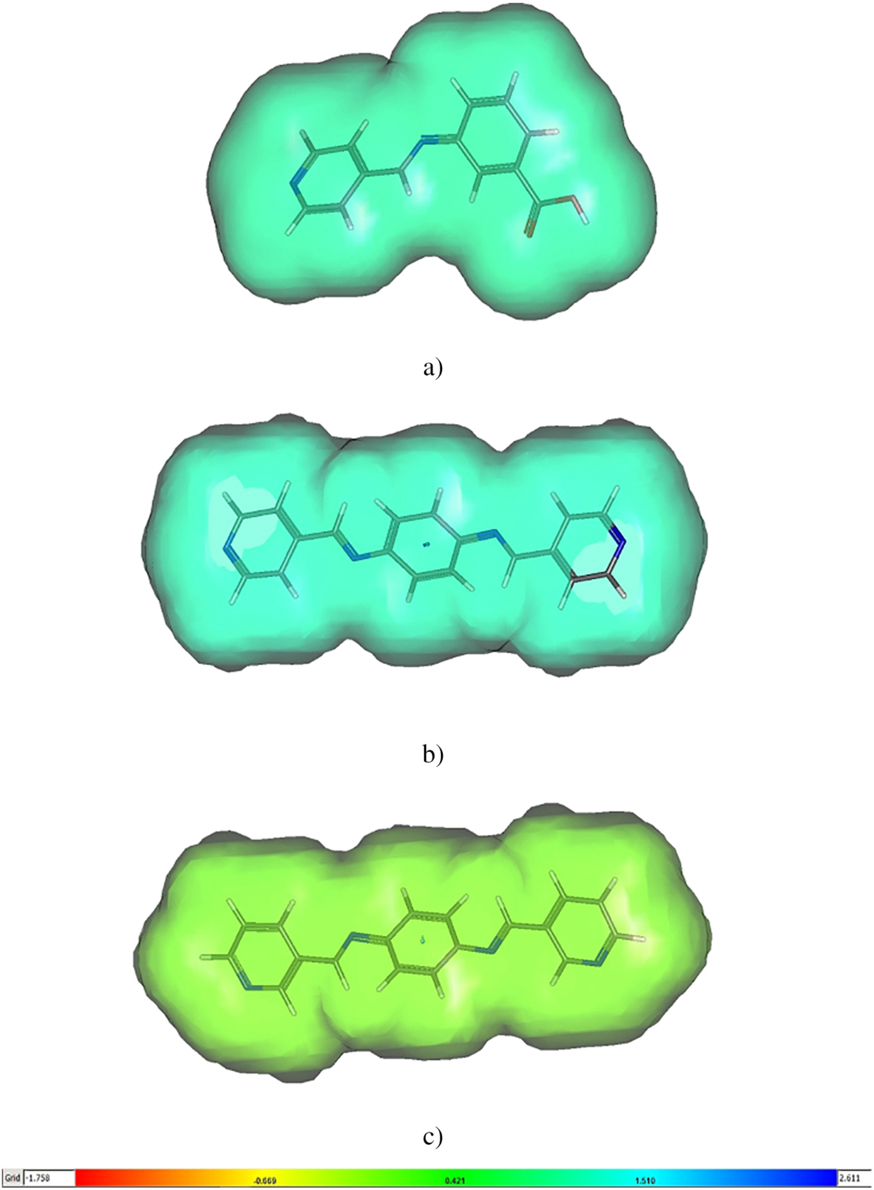

a)

b)

c)

Figure 3

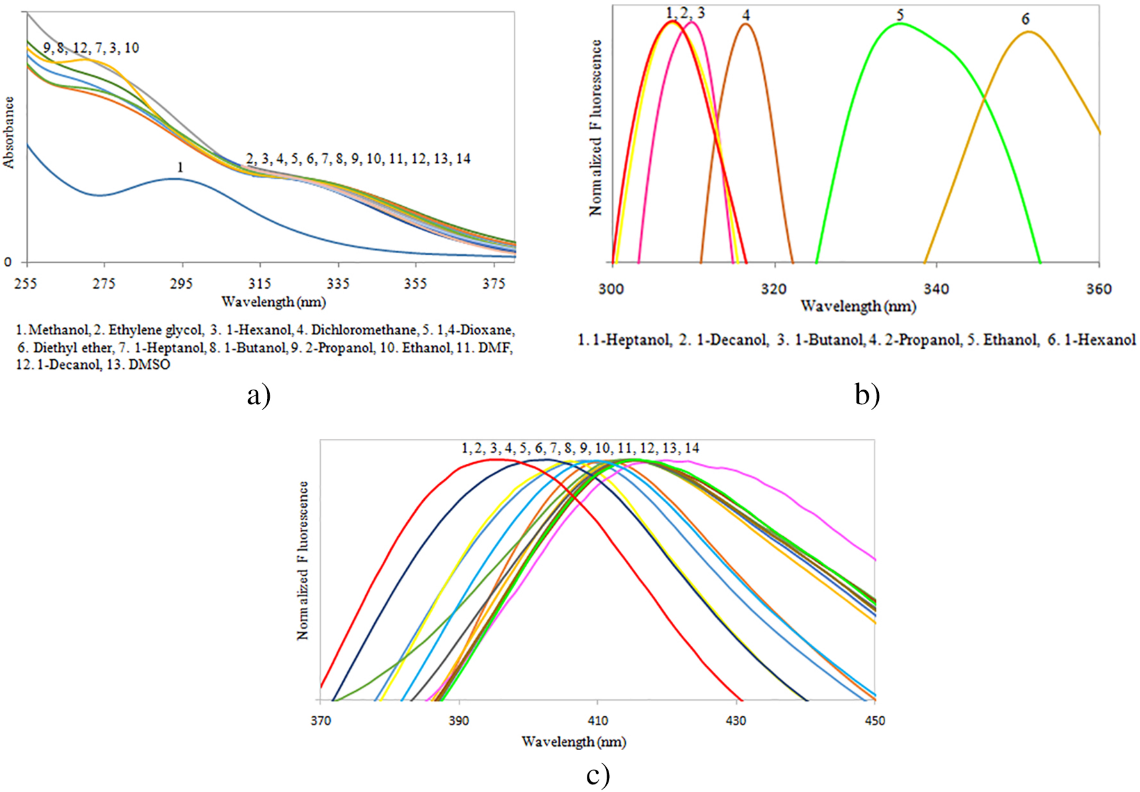
Absorbance
0
9, 8, 12, 7, 3, 10
2, 3, 4, 5, 6, 7, 8, 9, 10, 11, 12, 13, 14
1
255
275
295
315
335
355
375
Wavelength (nm)
1. Methanol, 2. Ethylene glycol, 3. 1-Hexanol, 4. Dichloromethane, 5. 1,4-Dioxane, 6. Diethyl ether, 7. 1-Heptanol, 8. 1-Butanol, 9. 2-Propanol, 10. Ethanol, 11. DMF, 12. 1-Decanol, 13. DMSO
a)
Normalized Fluorescence
1, 2, 3
4
5
6
300
320
340
360
Wavelength (nm)
1. 1-Heptanol, 2. 1-Decanol, 3. 1-Butanol, 4. 2-Propanol, 5. Ethanol, 6. 1-Hexanol
b)
Normalized Fluorescence
1, 2, 3, 4, 5, 6, 7, 8, 9, 10, 11, 12, 13, 14
370
390
410
430
450
Wavelength (nm)
c)

Figure 4

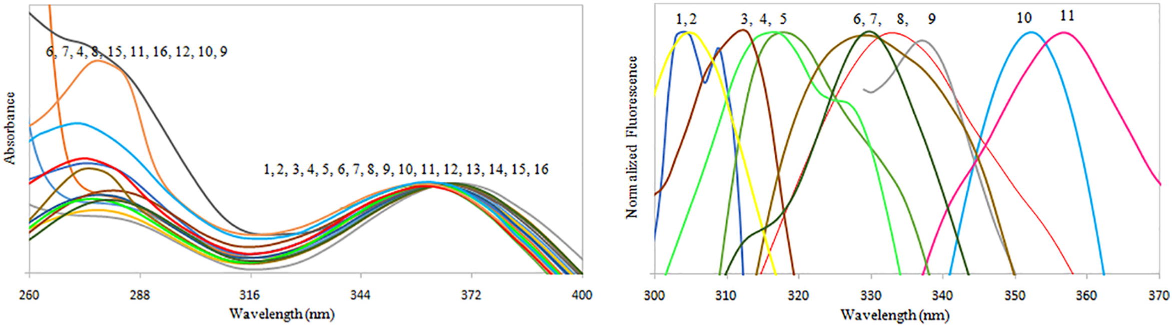

1. Water, 2. Diethyl ether, 3. 1,4-Dioxane, 4. Dichloromethane, 5. Acetone, 6. Cyclohexane 7. Ethanol, 8. Methanol, 9. DMF, 10. 1-Butanol, 11. 2-Propanol, 12. 1-Decanol, 13. 1-Heptanol 14. 1-Hexanol, 15. DMSO, 16. Ethylene glycol

a)

1. Decanol, 2. Methanol, 3. 1-Butanol, 4. 1-Propanol, 5. Ethanol, 6. Cyclohexane 7. Dichloromethane, 8. DMSO, 9. DMF, 10. Water, 11. Ethylene glycol

b)

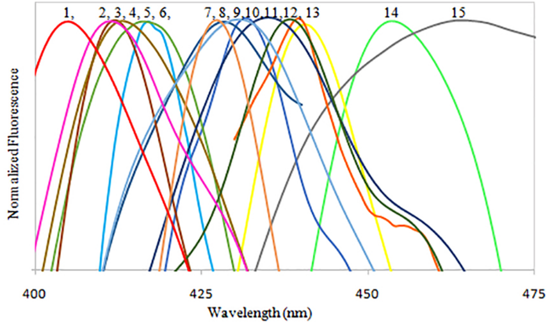

1. Cyclohexane, 2. 1,4-Dioxane, 3. 1-Propanol, 4. 1-Hexanol, 5. DMF, 6. Ethanol, 7. Diethyl ether, 8. 1-Decanol, 9. Acetone, 10. Methanol, 11. 1-Heptanol, 12. 1- Butanol, 13. Dichloromethane, 14. DMSO, 15. Water, 16. Ethylene glycol

c)

Figure 5

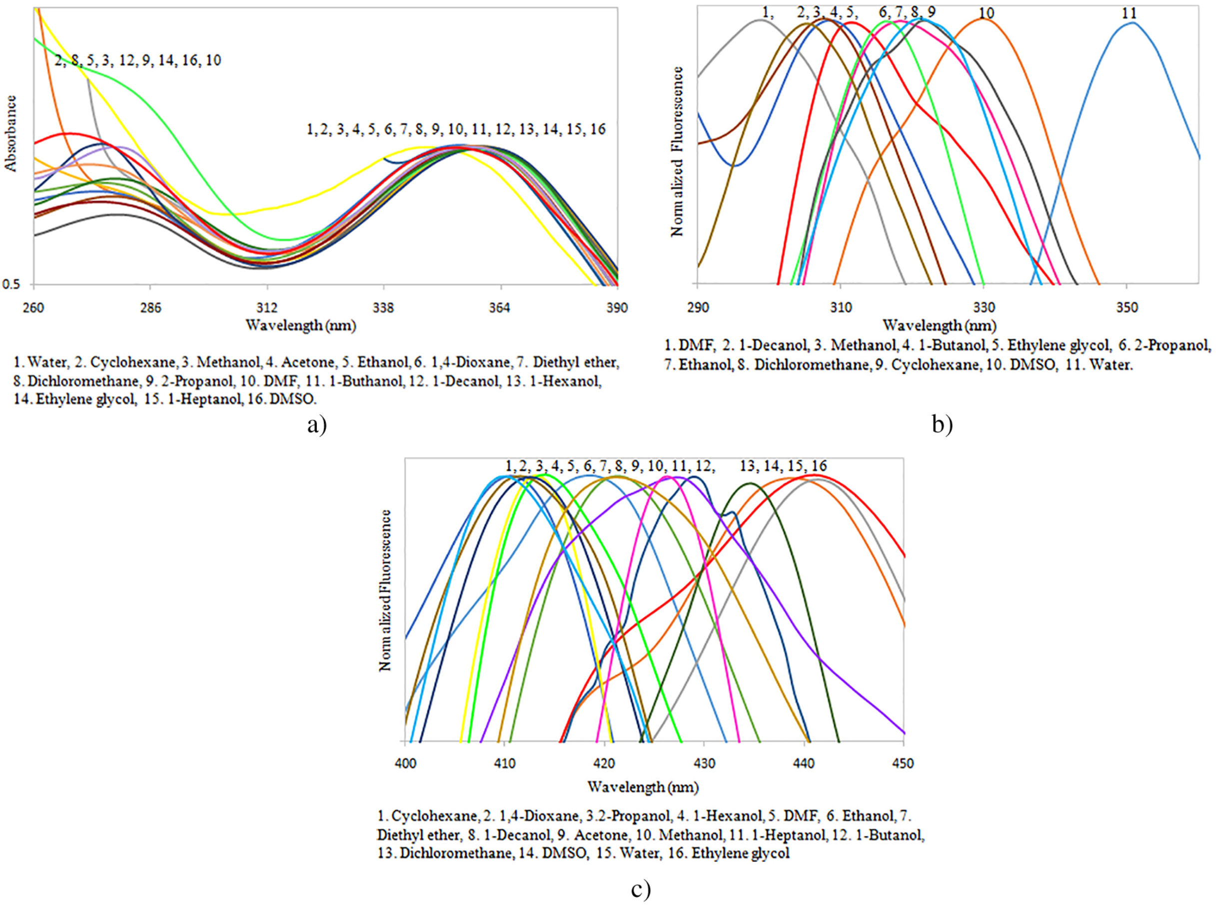
Absorbance
0.5
2, 8, 5, 3, 12, 9, 14, 16, 10
1, 2, 3, 4, 5, 6, 7, 8, 9, 10, 11, 12, 13, 14, 15, 16
260
286
312
338
364
390
Wavelength (nm)
1. Water, 2. Cyclohexane, 3. Methanol, 4. Acetone, 5. Ethanol, 6. 1,4-Dioxane, 7. Diethyl ether, 8. Dichloromethane, 9. 2-Propanol, 10. DMF, 11. 1-Buthanol, 12. 1-Decanol, 13. 1-Hexanol, 14. Ethylene glycol, 15. 1-Heptanol, 16. DMSO.
a)
Normalized Fluorescence
1,
2, 3, 4, 5,
6, 7, 8, 9
10
11
290
310
330
350
Wavelength (nm)
1. DMF, 2. 1-Decanol, 3. Methanol, 4. 1-Butanol, 5. Ethylene glycol, 6. 2-Propanol, 7. Ethanol, 8. Dichloromethane, 9. Cyclohexane, 10. DMSO, 11. Water.
b)
Normalized Fluorescence
1, 2, 3, 4, 5, 6, 7, 8, 9, 10, 11, 12,
13, 14, 15, 16
400
410
420
430
440
450
Wavelength (nm)
1. Cyclohexane, 2. 1,4-Dioxane, 3. 2-Propanol, 4. 1-Hexanol, 5. DMF, 6. Ethanol, 7. Diethyl ether, 8. 1-Decanol, 9. Acetone, 10. Methanol, 11. 1-Heptanol, 12. 1-Butanol, 13. Dichloromethane, 14. DMSO, 15. Water, 16. Ethylene glycol
c)

Figure 6

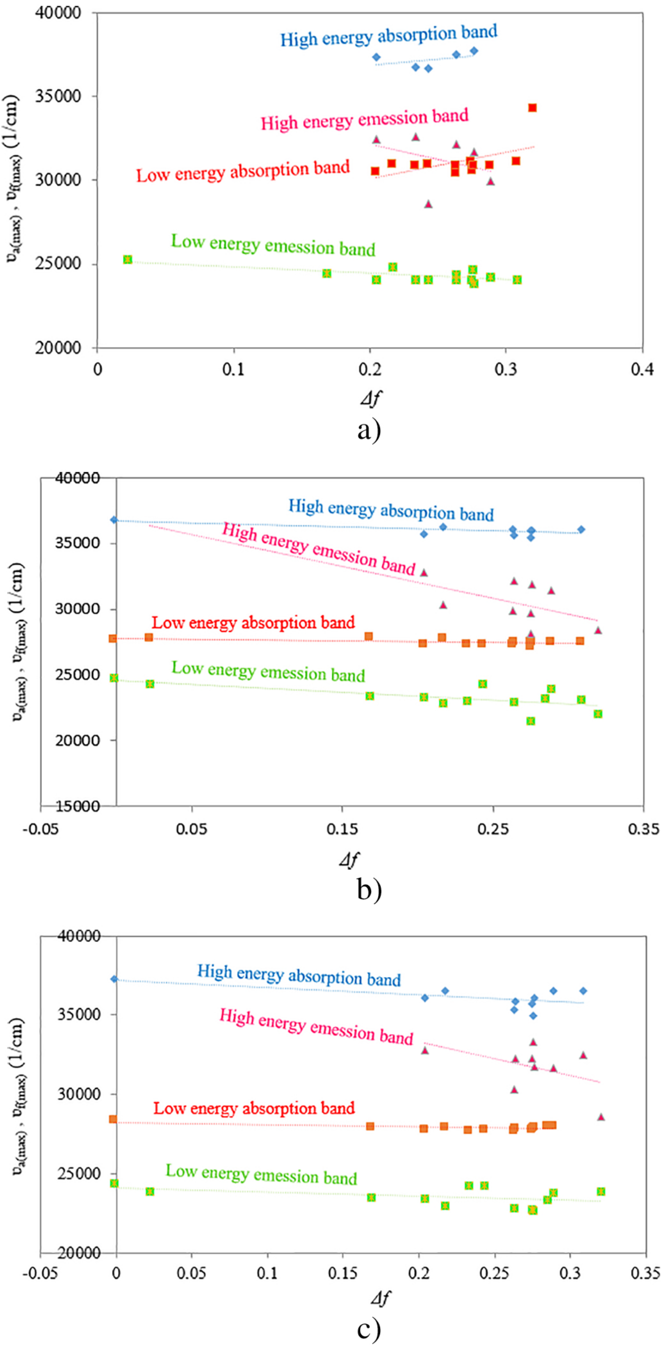

High energy absorption band
High energy emession band
Low energy absorption band
Low energy emession band
$\upsilon_{a(max)}$ , $\upsilon_{f(max)}$ (1/cm)
40000
35000
30000
25000
20000
15000
0
0.1
0.2
0.3
0.4
-0.05
0.05
0.15
0.25
0.35
Δf
a)
b)
c)

Figure 7

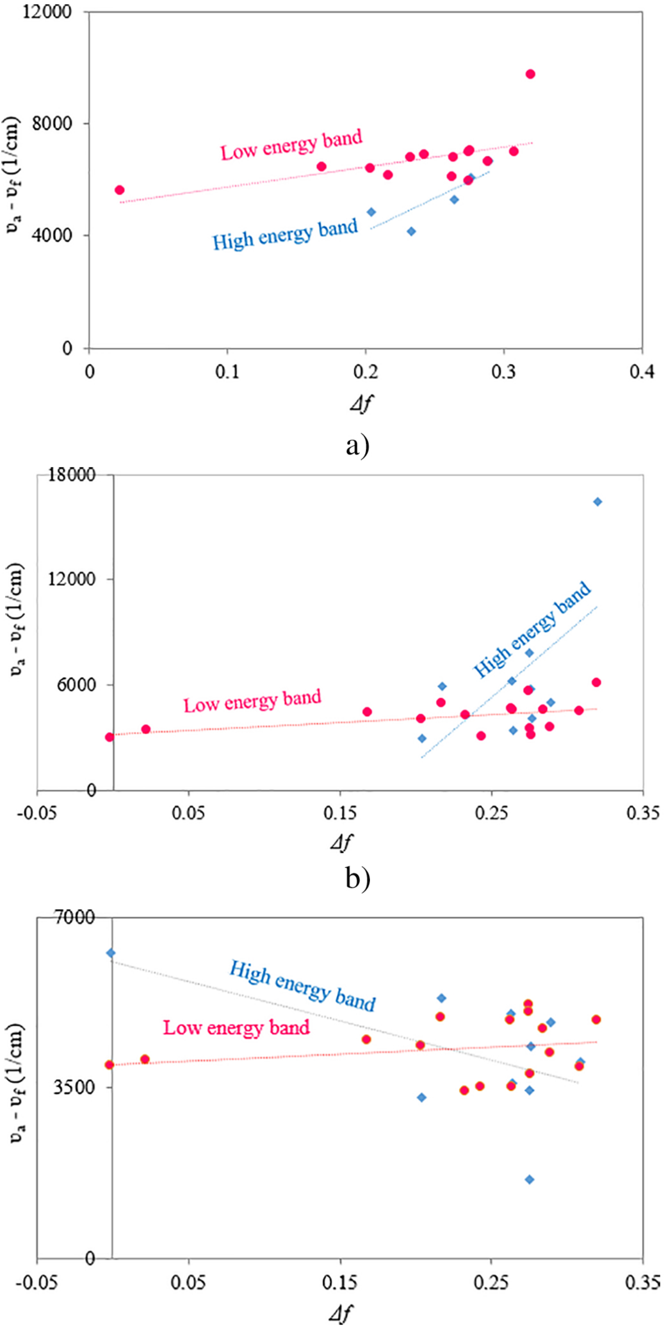
12000
8000
4000
0
$\upsilon_a - \upsilon_f$ (1/cm)
0
0.1
0.2
0.3
0.4
$\Delta f$
Low energy band
High energy band
18000
12000
6000
0
-0.05
0.05
0.15
0.25
0.35
7000
3500
0

a)

b)

c)

Figure 8

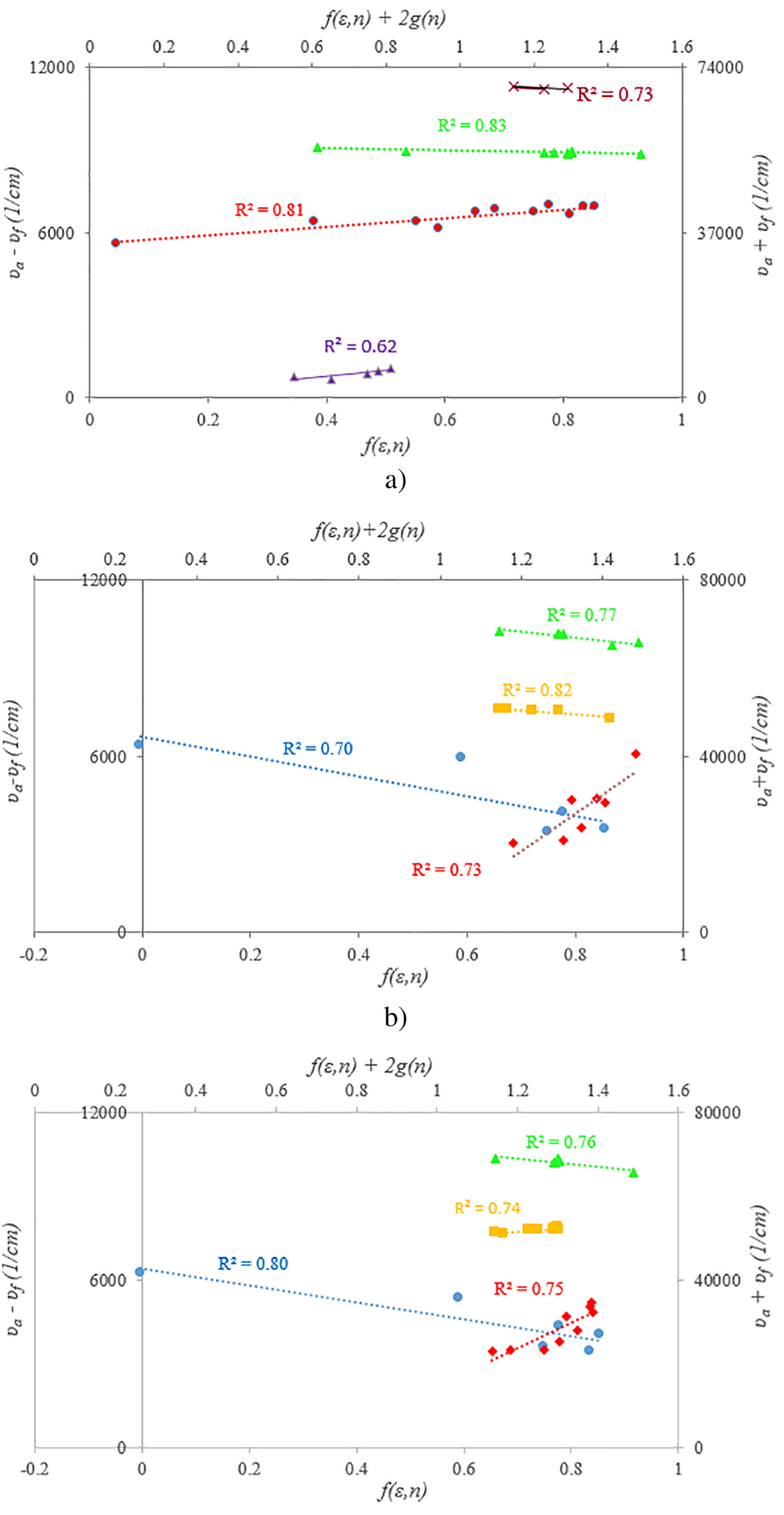
f(ε,n) + 2g(n)
0
0.2
0.4
0.6
0.8
1
1.2
1.4
1.6
12000
6000
0
74000
37000
0
$\upsilon_a - \upsilon_f$ (1/cm)
$\upsilon_a + \upsilon_f$ (1/cm)
R² = 0.73
R² = 0.83
R² = 0.81
R² = 0.62
0
0.2
0.4
0.6
0.8
1
f(ε,n)
f(ε,n)+2g(n)
0
0.2
0.4
0.6
0.8
1
1.2
1.4
1.6
12000
6000
0
80000
40000
0
$\upsilon_a - \upsilon_f$ (1/cm)
$\upsilon_a + \upsilon_f$ (1/cm)
R² = 0.77
R² = 0.82
R² = 0.70
R² = 0.73
-0.2
0
0.2
0.4
0.6
0.8
1
f(ε,n)
f(ε,n) + 2g(n)
0
0.2
0.4
0.6
0.8
1
1.2
1.4
1.6
12000
6000
0
80000
40000
0
$\upsilon_a - \upsilon_f$ (1/cm)
$\upsilon_a + \upsilon_f$ (1/cm)
R² = 0.76
R² = 0.74
R² = 0.80
R² = 0.75
-0.2
0
0.2
0.4
0.6
0.8
1
f(ε,n)

a)

b)

c)

Figure 9